

# A model of the chemical pathways leading to NO<sub>x</sub> formation during combustion of mixtures of cellulosic and plastic materials

T. Rogaume<sup>a,\*</sup>, J. Koulidiati<sup>b</sup>, F. Richard<sup>a</sup>, F. Jabouille<sup>a</sup>, J.L. Torero<sup>c</sup>

<sup>a</sup> *Laboratoire de Combustion et de Détonique, ENSMA, BP 40109, 86961 Futuroscope cedex, France*

<sup>b</sup> *Laboratoire de Physique et de Chimie de l'Environnement LPCE, Université de Ouagadougou, BP 7021, Ouagadougou 03, Burkina Faso*

<sup>c</sup> *School of Engineering and Electronics, The University of Edinburgh, Edinburgh, EH9 3JN, United Kingdom*

Received 16 August 2004; received in revised form 6 April 2005; accepted 4 July 2005

Available online 5 October 2005

## Abstract

A numerical model has been developed to study the NO<sub>x</sub> formation during the combustion of mixtures of cellulosic and plastic fuels within a fixed bed reactor. The model simplifies the flow to a one dimensional succession of about 1000 perfectly stirred reactors (PSR) and includes a detailed chemical model that computes 113 species involved in 893 reversible reactions, to detailed the reactive path of NO<sub>x</sub> formation. The calculations use the PSR model included in Chemkin II. The solid phase is not solved but instead the input species are generated from an experimental degradation study of the fuel. Nitrogen oxide (NO) is studied as the primary component of NO<sub>x</sub>. The model has been validated in past publication by comparison of the results with experimental measurements. The model has then been used to investigate the mechanisms of formation and destruction of the NO during the combustion process of municipal solid waste. Numerical results show that NO forms rapidly from the oxidation of intermediary species such as NCO, HNO and NH that originate from the fuel pyrolysis. NO consumption occurs primarily through reactions with NH<sub>3</sub> and NCO leading to the formation of N<sub>2</sub>. The ultimate formation and consumption of NO depends mostly on the primary air flowing through the fuel bed with a minimum being observed when primary air and fuel are present in proportions close to stoichiometric.

© 2005 Elsevier SAS. All rights reserved.

**Keywords:** Modelling; Kinetic mechanisms; NO<sub>x</sub>; Incineration; Municipal solid wastes

## 1. Introduction

Incineration is one of the most commonly employed techniques of treatment of Municipal Solid Waste (MSW) in Europe, mainly because it allows a reduction of 70% of the mass and 90% of the volume of the waste. However, the biggest challenge for incineration remains on the transfer of pollution from the waste to the air, either through gaseous emissions or ashes.

Among the major environmental concerns related to incineration are the emissions of nitrogen oxides (NO<sub>x</sub>) that have been shown to strongly contribute to the formation of acid rain and photochemical smog [1]. During the incineration of municipal solid waste in grid furnace incinerators, NO is the major component of the NO<sub>x</sub> formed, representing 95% of those emissions [2]. Therefore, it is justifiable to concentrate only on the

establishment of the main variables controlling NO. Incinerator temperatures are in the range of 1173–1323 K [3], and combustion is generally lean, as shown by typical residual oxygen levels comprised between 6 and 12%, therefore the quantity of NO formed by means of the thermal and prompt mechanisms can be considered negligible [4]. The main formation path, responsible for more than 95% of the nitrogen monoxide produced during incineration of MSW is through the fuel-NO mechanism [5]. Thus modifications of the combustion processes bear a great potential for reducing NO<sub>x</sub> emissions.

For a successful application of the different primary techniques of reduction, the governing parameters must be evaluated very carefully and the knowledge of the kinetic mechanism of NO formation must be known precisely. The formation of NO from the fuel has been well described for the combustion of different materials [6,7] but not for heterogeneous mixtures of materials such as cellulose and plastics such as municipal waste. The nitrogen from HCN and from NH<sub>3</sub> have been

\* Corresponding author. Tel.: +33 549 49 82 90; fax: +33 549 49 82 91.  
E-mail address: [trogaume@dug.chanzu.univ-poitiers.fr](mailto:trogaume@dug.chanzu.univ-poitiers.fr) (T. Rogaume).

identified as the two main sources for  $\text{NO}_x$  and on the basis of this premise general mechanisms of formation of NO have been proposed [7]. Furthermore, the particular paths for NO formation have been linked to fuel properties through the devolatilisation products [7].

Application of this type of mechanisms and methodologies to the incineration of MSW has not been addressed in detail. Furthermore, optimisation of the combustion process in order to reduce the gaseous emissions requires detailed knowledge of the principal reactive zones within the furnace. This information remains unavailable for MSW incinerators. In an attempt to fill this gap, Rogaume et al. [8] presented a description of the reactive zones for a fixed bed incinerator of a fuel mixture representative of MSW. Based on this experimental study a numerical model was developed and used to predict different pollutant species [9,10]. Good agreement between numerical and experimental results served as validation to the model. Here, the same model is used to establish the different reaction mechanisms leading to the formation and destruction of  $\text{NO}_x$  and their relationship with the different reaction zones. A sensitivity analysis is carried by systematically varying the oxidizer supply to the reaction, through the fuel (primary air) and later into the gas phase combustion region (secondary air).

## 2. The combustion model

The architecture of the model has been presented in detail in Rogaume et al. [9,10] and only a brief summary will be presented here. The model permits the simulation of the combustion process within a counter flow fixed bed reactor. A schematic of the reactor is presented in Fig. 1. Details on the reactor characteristics and experimental procedures can be found in Rogaume et al. [8]. Direct study of MSW poses significant problems because of its heterogeneous nature and the complexity and toxicity of some of its minor components. Therefore, here only the main components have been used (wood, cardboard, PET and polyamide) and are mixed in proportions consistent with those found in MSW: 41% of wood, 37% of cardboard, 19% of PET and 3% of polyamide.

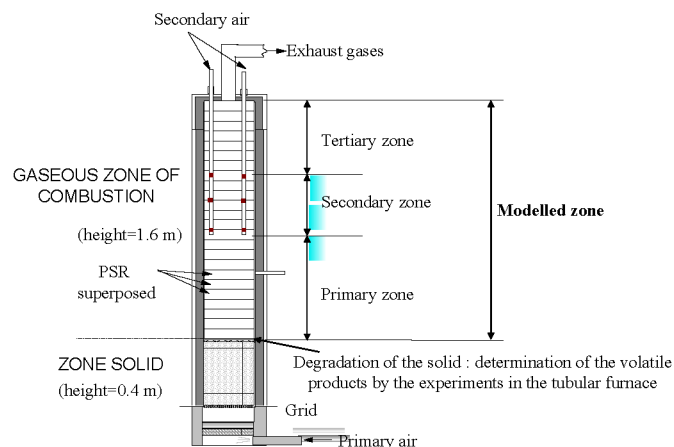


Fig. 1. Schematic of the reactor indicating the basic structure used for the model.

It is usually assumed that combustion of MSW can be divided into three steps [8,11]; degradation of the waste, combustion of volatile gases and char burnout. Rogaume et al. [8] showed that for the present fuels, degradation could be considered as pure pyrolysis with little or no heterogeneous oxidation present. The combustion of the volatile gases takes place in three different reactive zones: the primary zone where the products of pyrolysis burn with the primary air, from the top of the solid bed to the secondary zone, the secondary zone, where the products issue from the primary zone burn with the secondary air (introduced through ports axially distributed), and a tertiary zone or cool down region where the combustion ends. Past studies have demonstrated that char burnout is negligible for these particular fuels [8,9], in our conditions. For modelling purposes fuel intake will be defined by pyrolysis and char burnout will be neglected and only the gas phase combustion will be described.

Detailed modelling of both chemistry and transport is of extreme complexity for these reactors and generally requires long computations. The benefit of this type of models is nevertheless not clear since the assumptions, related to both transport and kinetics, tend to be very strong. Since the main objective of the study is  $\text{NO}_x$  formation, emphasis is given to combustion chemistry and a simplified approach to the flow is introduced.

Antifora et al. [12] reveal that in the case of nitrogen oxide formation reactions, a detailed chemistry is needed. Furthermore, Vitali et al. [13], working on the optimisation of re-burning via modelling, demonstrated that a detailed chemical mechanism with a simplified representation of mixing could be used not only to explore the chemistry process but also to identify ranges of process parameters that give optimum performance. This approach requires embedding all the necessary detail in the chemistry of formation/reduction of the  $\text{NO}_x$ . On the basis of these conclusions, a detailed and comprehensive kinetic model is applied to a network of ideal reactors built to approximate in one dimension, the three-dimensional flow field within the furnace. The literature sites further examples where this approach has been privileged to predict formation of  $\text{NO}_x$  [11–14].

The reactor is broken into a multitude of separate disks where the input of one is the output of the one upstream as shown in Fig. 1. Transport will be simplified to a one-dimensional flow and turbulence will be assumed to be homogeneous within each reactor. Each reactor can be then considered as an adiabatic Perfectly Stirred Reactor (PSR). This construction of the model is similar that the use of plug flow reactor, but it permits to take into account the injection of the secondary air, what is not possible with a plug flow. The chemistry occurring within the reactor is established using Chemkin II [15]. Several kinetic models have been developed to study NO formation in conditions similar to the present ones [7,16,17]. In this work, due to the composition of the gases introduced by pyrolysis, the detailed kinetic model proposed by Dagaut et al. [18], and composed by 112 species involved into 892 reversible reactions was used. Justification of this choice and the addition of a dissociation reaction for  $\text{CH}_3\text{CONH}_2$  (which is a product of the pyrolysis of polyamide) has been described elsewhere and will not be detailed here [9,19]. The computer program

was developed to make use of Chemkin II [15] with the PSR model [20]. The model requires the definition of a local temperature, for this purpose experimental values have been used as input values [8]. All results were obtained with at least 1000 PSR being deemed as sufficient resolution to obtain independence of the results from this parameter and to optimize time of calculation.

For initialisation the program requires the knowledge of the volatile products generated by the thermal degradation of the solid. This composition, which formed the initial condition to start the simulation in the first PSR has been obtained experimentally using a tubular furnace [9]. To complete the reconstruction of the components that could not be measured, values from the literature have been incorporated. The complete reconstruction of the 1400 grams of fuel present in the reactor is presented in molar percentage. The composition of the products of pyrolysis assumed to be 35.75% of CO, 5% of CO<sub>2</sub>, 12.8% CH<sub>4</sub>, 9% C<sub>6</sub>H<sub>6</sub>, 0.18% CH<sub>3</sub>CONH<sub>2</sub>, 0.4% HCN, 0.1% NH<sub>3</sub>, 0.03% NO, 13.7% H<sub>2</sub>, 0.23% HNCO, 22.9% OH. Details on the methodologies and procedures are presented in Ref. [9]. Too much information that is needed to assess this work is presented in past papers [9].

### 3. Results

#### 3.1. Validation of the model

The numerical model was benchmarked against a series of experimental results [8]. The measured NO concentrations show good agreement with the model for  $e_T \leq 2$  (Fig. 4). For  $e_T > 2$  the model over predicts the NO concentration for the lower values of the primary air, the production of NO seems to be better estimated for  $e_1 = 1.8$ . The numerical model uses the kinetic model developed by Dagaut et al. [16] which has been validated for an equivalence ratio between 0.7 to 2.5, therefore it is not surprising that when the overall equivalence ratio goes below 0.5 ( $e_T = 2$ ) that errors can arise. These errors seem to be magnified when the local equivalence ratio in the secondary zone of combustion decreases keeping this region well below the minimum equivalence ratio for with the kinetic model has been validated. The symbols mod. represent the obtained with the model and the symbols exp. referred to the experimental results. (See Fig. 2.)

The results for the residual oxygen concentration are presented in Fig. 3. The symbols mod represent the obtained with the model and the symbols exp. referred to the experimental results. As expected, the amount of oxygen left over increases with the excess air in an almost linear fashion. The model predicts very well the trends but nevertheless consistently over predicts the oxygen concentration by about 15%. The over prediction could be attributed to the oxidation of the combustion products between the reactor and the analyzer. Temperatures at the exit of the reactor, which corresponds to the modeling domain, are still high and further oxidation can be expected.

The concentrations of CO<sub>2</sub> are presented for  $1.7 \leq e_T \leq 2.4$  in Fig. 4. The range of excess air presented was limited to the conditions most commonly employed during the incineration of

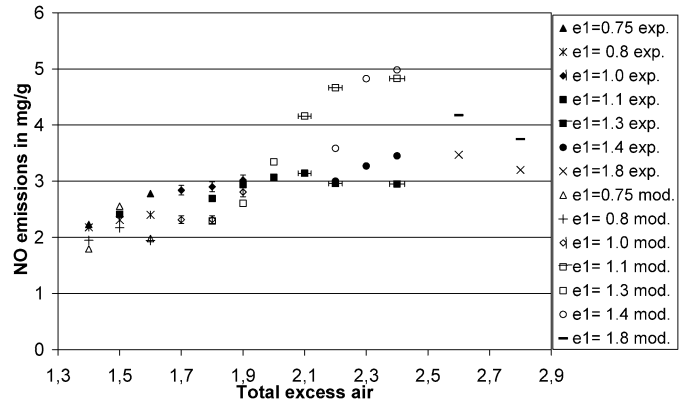


Fig. 2. Comparison of the measured and predicted NO profiles as a function of the total excess air for different values of the primary excess air ( $e_1$ ). exp.: measured point, mod: predicted.

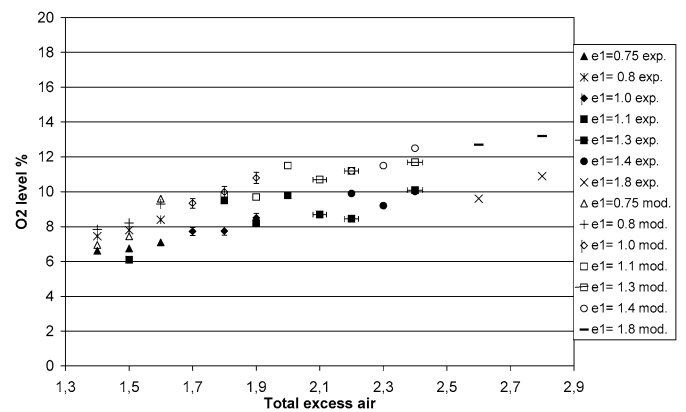


Fig. 3. Comparison of the measured and predicted residual oxygen concentration at the exit of the reactor and as a function of the total excess air for different values of the primary excess air ( $e_1$ ). exp.: measured point, mod: predicted.

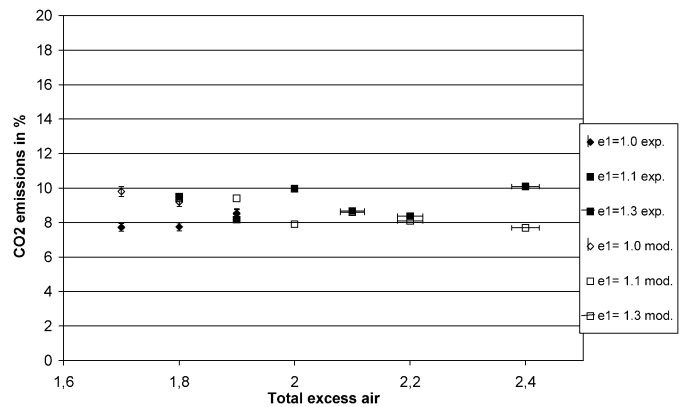


Fig. 4. Comparison of the measured and predicted CO<sub>2</sub> concentrations at the exit of the reactor and as a function of the total excess air for different values of the primary excess air ( $e_1$ ). exp.: measured point, mod: predicted.

municipal solid wastes. The results show good agreement between the measured CO<sub>2</sub> concentrations and the model, particularly for  $1.8 \leq e_T \leq 2.2$ . As expected, no systematic influence of the primary air on the results could be observed. Furthermore, CO<sub>2</sub> concentrations remain almost constant indicating that, within the range of flow rates studied, carbon oxidation is

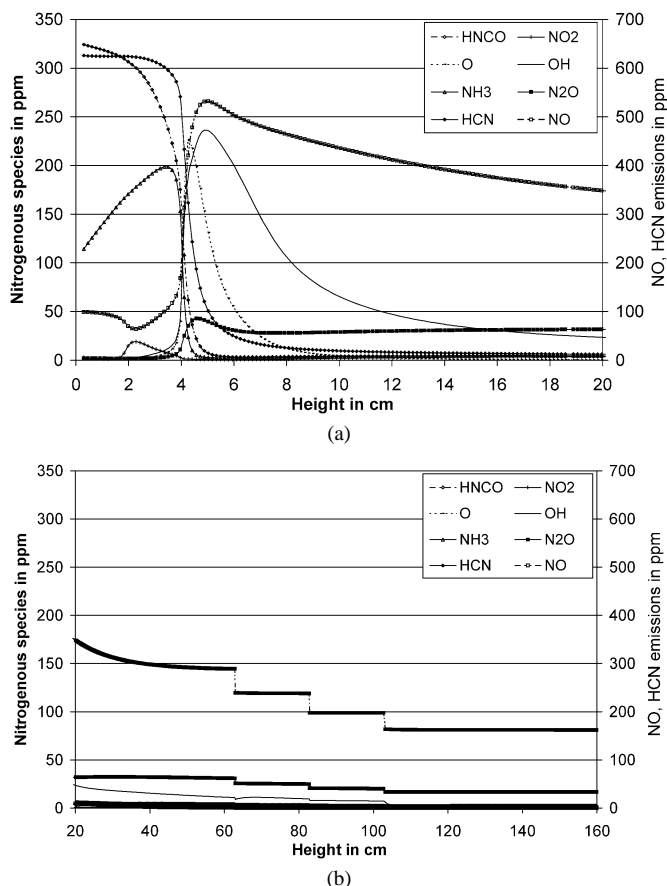


Fig. 5. Typical evolution of (a) the nitrogenous species across the reactor between the top of the solid bed to 20 cm up and (b) between 20 cm to the top of the bed to the exhaust. Combustion occurs with a primary airflow of  $Q_1 = 50 \text{ N}\cdot\text{m}^3\cdot\text{h}^{-1}$  (corresponding to a primary excess air,  $e_1 = 1$ ) and a secondary airflow of  $Q_2 = 35 \text{ N}\cdot\text{m}^3\cdot\text{h}^{-1}$  (corresponding to a secondary excess air,  $e_2 = 0.7$ ).

not limited by oxygen supply but by the kinetics of the reaction and that the oxygen concentration into the furnace is sufficient to have a quasi-complete combustion. The symbols mod represent the obtained with the model and the symbols exp. referred to the experimental results.

### 3.2. Evolution of the nitrogenous species

To be able to identify the important reaction pathways it relevant to track the evolution of the different species in the context of the different reactions involved. The structure of the model allows the possibility of determining the gas composition at the output of each PSR providing a mapping along the reactor.

Figs. 5(a) and 5(b) show the evolution of nitrogenous species along the reactor for a representative condition of combustion. The species shown are only those that are expected to play a significant role in the production of NO. Omitted from the plot are NCO, NH, HNO and  $\text{NH}_2$  that are also recognized as important intermediary species to the production of NO. These radicals are not presented because their destruction rates are similar to their production rates, thus, cannot be tracked.

Fig. 5 demonstrates that a first reacting zone is identified between the fuel degradation surface (height = 0 cm) and 10 cm

above. Consumption of the products of pyrolysis (HCN, HCNCO and  $\text{NH}_3$ ), in majority by oxidation, occurs in this zone. It can be seen that initially HCN and HCNCO are consumed slowly ( $\leq 3$  cm). During this time, the concentration of  $\text{NH}_3$  increases due to the decomposition of  $\text{CH}_3\text{CONH}_2$ . The increase in concentration of O and OH radicals results in the consumption of HCN, HCNCO and  $\text{NH}_3$  leading to the production of NO,  $\text{N}_2\text{O}$  and  $\text{N}_2$  [7]. This zone corresponds to the formation of NO and the pertinent reactions take place quickly early on, between 3 and 6 cm (Fig. 5).  $\text{NH}_3$  is oxidised faster than HCNCO, with HCN being the last one to be consumed. It is important to notice that NO is formed more rapidly than  $\text{N}_2\text{O}$  and  $\text{N}_2$  and it will only react later to form  $\text{N}_2\text{O}$  and  $\text{N}_2$ . The concentration curve for  $\text{N}_2\text{O}$  is presented in Fig. 2(a) but that for  $\text{N}_2$  has been omitted for clarity of presentation. It is important to note that even after NO formation ( $> 5$  cm) HCN and HCNCO are not totally consumed. The  $\text{N}_2$  and  $\text{N}_2\text{O}$  concentration curves follow the same trend, but concentrations are much higher thus will distort the scale of the plot. The oxidation of the different products to go to NO is achieved mostly with the radical O, and of lesser importance, with the radicals OH and H. The NO coming directly from the degradation of the combustible is directly oxidized to form  $\text{NO}_2$  that will further react to form other combustion products.

In a second zone, between 10 and 63 cm, the concentration of the different intermediates are low, and their role negligible. Once HCN and HCNCO have been fully consumed a double path for the slow destruction of NO follows. On the one hand oxidation leads primarily to the production of  $\text{N}_2$  but also, to a lesser extent, to the production of  $\text{NO}_2$ . The reduction of the NO concentration takes place until the injection of the secondary air.

The injection of the secondary air is staged in three levels located respectively at 63, 83 and 103 cm. The description of the profile of evolution of the species allows the identification of a third reaction zone. Eventually, the concentrations of  $\text{NO}_2$  and  $\text{NH}_3$  start to decrease while the NO concentration attains a steady value. Indeed, in a first step, the injection of the secondary air contributes slightly to the formation of  $\text{N}_2$  and consequently to a reduction of the emissions of NO. The step changes in concentration occurring at this stage are due to dilution brought by the injection of air.

After the third injection port the different species concentrations do not evolve anymore identifying the end of the combustion.

As mentioned before, the information presented in Fig. 5 does not allow studying the intermediate radicals (NH, HNO and  $\text{NH}_2$ ) of proven importance to the formation of NO [7]. Furthermore, it does not allow describing the species that will react and reduce NO. It is therefore necessary to study the reaction mechanisms of NO formation. The PSR model gives as output the rates of all chemical reactions within the combustion mechanism. Therefore it is possible to determine the evolution of particular species from the calculation of the global rates of formation and consumption. The construction of the chemical pathways has been done using those global rates at each step of the reaction. The output rates for 50 specific PSR, chosen at critical locations from diagrams such as Fig. 5, have been

used to follow the nitrogenous species. Tracing the NO path it is possible to determine the principal intermediates and reactions leading to its formation or destruction and to back track these steps until reaching the original products of pyrolysis and inert species. This allows the construction of a reaction path for the formation and consumption of NO.

#### 4. Reactive path analysis

Fig. 6 identifies the reacting path for the formation of NO as developed following the methodology presented above. Fig. 6 shows that NO is formed from the nitrogen contents of the fuel through three main steps. First, pyrolysis of the waste leads to the formation of HCN, NH<sub>3</sub>, HNCO and CH<sub>3</sub>CONH<sub>2</sub> (and directly a small part of NO). These species appear on Fig. 5(a) at height equal 0. Then, those components react to form the principal intermediates that are NCO, NH and HNO.

- HNCO conduct directly to the formation of NCO and reacts to form NH<sub>2</sub> and than NH;
- HCN is oxidised to form NCO directly or through the formation of the radical CN and

- NH<sub>3</sub> reacts to form NH<sub>2</sub> that will lead to the formation of NH and HNO.

The reactions take place in the previously described first zone and occur principally with the radicals O, OH and H which originate mainly from the dissociation of the oxygen and the water. Finally, NCO, NH and HNO will lead to the formation of NO. Equilibrium conditions between NO and NO<sub>2</sub> can be observed in this zone.

It is important to note the preponderance of the radical O, which highlights the importance of the local concentration of oxygen and thus the primary air. This result is in accordance with the description of the yield of formation of the NO through the fuel mechanism described by De Soete [4]. During this phase of NO production, part of the NO formed is converted to N<sub>2</sub>. Nevertheless, the rate of consumption of NO is less important than its rate of production. We remark that N<sub>2</sub> is not formed directly from the products of degradation, but is formed from the NO.

In a similar manner it is possible to establish the chemical mechanism of consumption of NO. The corresponding reactive schema is presented in Fig. 7. NO is principally consumed by NH<sub>2</sub>, NH and NCO to form molecular nitrogen. This consump-

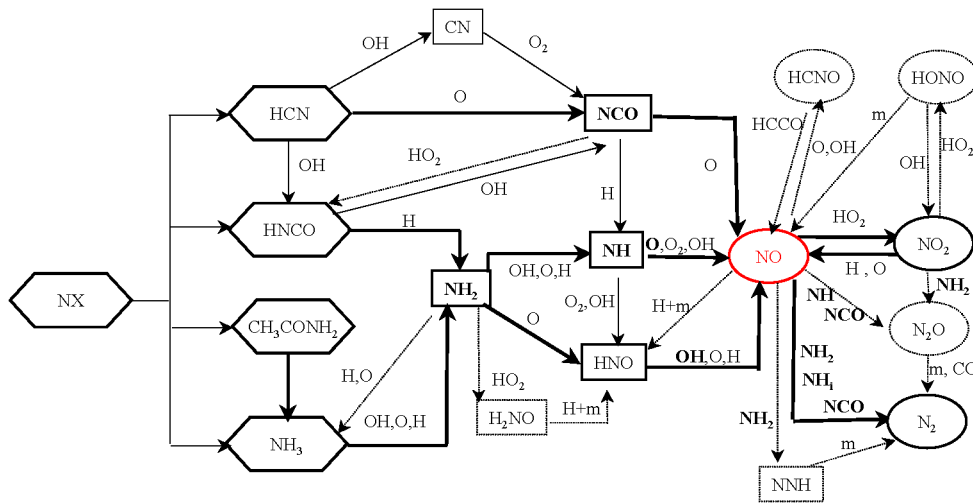


Fig. 6. Reacting path analysis of formation of NO and N<sub>2</sub>.

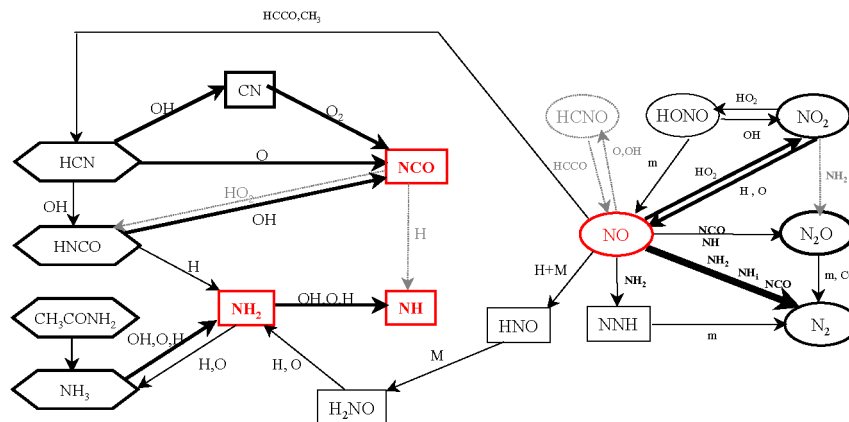


Fig. 7. Reacting path analysis of consumption of the NO.

tion is done directly or through the formation of NNH and  $N_2O$ . NO can also react with HCCO and  $CH_3$  to generate HCN or conduct to the formation of  $NH_2$  through reaction with HNO and  $H_2NO$ . The choice of the reducing pathway and the yield of reduction is dependant of the excess air of combustion.

The schema of NO destruction is quite simple but it is important to identify how the reducing species are generated. The reducing species are formed by three mechanisms illustrated in Fig. 7:

- Initially, NCO is generated by the oxidation of HNCO and HCN. This oxidation can be direct or through the intermediate species CN.
- Then,  $NH_2$  and NH appear as products of the oxidation of ammonia or from the reduction of NO. Ammonia originates from the fuel degradation and from the dissociation of  $CH_3CONH_2$  (Fig. 6). It is important to note that  $NH_2$  and NH can also form HNO, which in turn is oxidised to form NO, but the rate of this reaction is low.
- HCCO and  $CH_3$  come from the reaction of the hydrocarbons species.

NO remains in equilibrium with  $NO_2$  but the equilibrium condition is directly dependent on the oxygen concentration. An increase of the oxygen concentration favours the formation of NO. The formation of the different species participating in the destruction of NO is primarily dependent on the concentration of the OH radical.

In summary, the final product of the oxidation of nitrogenous compounds is  $N_2$ , which according to the schemas above, is formed by the reduction of NO. The main reactions leading to the formation of NO occur in the first combustion zone, close to the fuel surface, and are highly dependent on the presence of the O radical. Thus the oxygen concentration in this region, and thus the primary air, appears to be the critical parameter influencing the formation of NO. Transformation of NO into  $N_2$  depends on the primary excess air and will occur through the intermediary species  $NH_2$ , NH and NCO and will occur mainly in a second combustion zone preceding the region of secondary air injection (10–103 cm). The formation of these species is strongly influenced by the oxygen concentration. A high oxygen concentration will lead to a weak presence of the intermediary species. So, for the second reaction zone; high oxygen concentration will lead to the inhibition of NO reduction. Formation and reduction of NO can thus be directly linked to the primary air.

The present results concentrate on conditions where the primary air is greater than the stoichiometric requirement. But, numerical results also show that in the event that the primary air is smaller than stoichiometric the main reaction front is displaced towards the first secondary air injection port where NO is mostly formed following the same paths as indicated above. Under these conditions, the low temperatures in this zone of the reactor hamper NO reduction.

## 5. Influence of primary and secondary air

Fig. 8 compares NO emissions against primary and secondary excess air. A set of experimental results is presented together with numerical results corresponding to the experimental conditions. There is good agreement between calculated and experimental results. A parametric study of the reaction zone temperatures ( $T_1$ ,  $T_2$ ) and the fuel consumption rate is also included in Fig. 8. It is important to reiterate that the values of the fuel consumption rate and the temperatures for both reaction zones ( $T_1$ : primary zone of combustion,  $T_2$ : secondary zone of combustion) are obtained from the experimental data. Fixing these three parameters deviate the conditions from those observed experimentally, since the burning rate and the temperatures are functions of the excess air. Nevertheless, this limited parametric study provides a sense of the independent effects of each variable.

It is necessary to clarify that changes in the primary airflow will have an impact on the fuel consumption rate and on

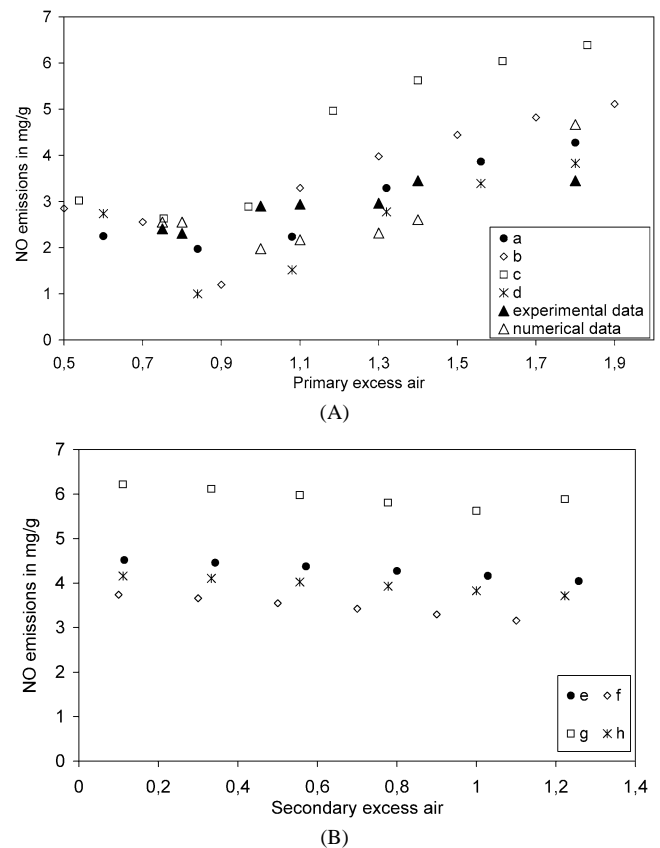


Fig. 8. (A) Influence of the primary excess air, (B) influence of the secondary excess air on the formation of NO for four different experimental conditions. All emissions are given in mg of pollutant/gram of fuel burnt.  $T_1$  represents the average temperature in the primary zone of combustion,  $T_2$  in the secondary zone and  $t_c$  the time to total fuel consumption. (a)  $e_2 = 0.8$ ,  $T_1 = 1213$  K,  $T_2 = 1213$  K and  $t_c = 540$  seconds. (b)  $e_2 = 0.9$ ,  $T_1 = 1233$  K,  $T_2 = 1283$  K and  $t_c = 485$  seconds. (c)  $e_2 = 1$ ,  $T_1 = 1293$  K,  $T_2 = 1303$  K and  $t_c = 500$  seconds. (d)  $e_2 = 1$ ,  $T_1 = 1203$  K,  $T_2 = 1273$  K and  $t_c = 520$  seconds. (e)  $e_1 = 1.8$ ,  $T_1 = 1213$  K,  $T_2 = 1213$  K and  $t_c = 540$  seconds. (f)  $e_1 = 1.1$ ,  $T_1 = 1233$  K,  $T_2 = 1283$  K and  $t_c = 485$  seconds. (g)  $e_1 = 1.4$ ,  $T_1 = 1293$  K,  $T_2 = 1303$  K and  $t_c = 500$  seconds. (h)  $e_1 = 1.8$ ,  $T_1 = 1203$  K,  $T_2 = 1273$  K and  $t_c = 520$  seconds.

the temperatures of both the zones of air injection. In contrast, changes in the secondary airflow will affect only the temperature of the zone of secondary air injection. The complex and uneven nature of the couplings makes it impossible to separate one parameter while keeping all others constant, thus the need to limit the parametric study.

Four sets of conditions based on experimental data are presented. The corresponding excess air is varied and the evolution of NO is described. Fig. 8 shows the evolution of the NO concentration at the outlet of the reactor as a function of the primary air (A) and the secondary air (B). The study of the influence of the primary excess air has been done keeping the secondary excess air constant and inversely for the study of the influence of the secondary excess air. It can be observed that the NO production decreases with the primary air for  $e_1 < 1$ , an inflection point occurs at  $e_1 \approx 1$  and from then on the NO concentration increases almost linearly with  $e_1$ . This trend is consistent for all conditions modelled. For  $e_1 < 1$  it can be observed that all the data collapses to one single curve indicating that under these conditions temperature has a minor effect on the production of NO, the controlling mechanism clearly being the availability of oxygen. An increase in the secondary air seems to have little effect on the inflection point and on the total NO production for  $e_1 < 1$ . Fig. 8(B) shows data for  $e_1 > 1$ . For  $e_1 > 1$  highest NO production is given for condition (g) and the lowest for condition (f). The influence of  $T_1$  is thus evident when a surplus of oxygen is available. Conditions in the zone of secondary air injection seem to have only a minor effect on the ultimate NO concentrations.

- (a) The evolution of the NO production with the secondary airflow demonstrates that no change of combustion regime can be observed indicating that the two zones observed previously are only a function of the primary airflow. Furthermore, it can be seen that if the temperatures in the reaction zones remain constant, NO production is somehow insensitive to the oxygen concentration in the secondary zone of combustion. This observation is in contradiction with the experimental observations, thus providing evidence that temperatures in the zone of secondary air injection do have a role in the ultimate concentration of NO. The temperature of the secondary zone of combustion is increased with the secondary airflow, and consequently the NO concentration.

## 6. Conclusions

A computational model was developed to study the production of pollutants during the incineration of a fuel mixture that resembles urban waste. The results of the model have been compared with experiments conducted in a fixed-bed reactor that allows for primary and secondary air injection. Experimental results and model predictions showed good qualitative agreement.

The numerical model has been used to establish the primary chemical pathways and their occurrence at each specific location within the reactor. It can be concluded that NO formation occurs primarily just above the fuel degradation front (between

the top of the bed and 12 cm above) and its rate is defined by the presence of the radicals O, OH, and H. The formation of NO from the fuel can be divided into three different steps:

- The pyrolysis of the combustible generates the production of HCN, NH<sub>3</sub>, HNCO, CH<sub>3</sub>CONH<sub>2</sub> and a small amount of NO. CH<sub>3</sub>CONH<sub>2</sub> will dissociate itself to form NH<sub>3</sub>.
- HCN, NH<sub>3</sub>, HNCO react with the radicals, to form the principal intermediates of the formation of NO that are NCO, NH and HNO. This step takes place between 6 and 10 cm above the combustible. It is important to note the importance of the local oxygen concentrations for this step through the O radical.
- NCO, NH and HNO react to form NO.

The reactions of formation of NO are quite dependant of the local concentration of oxygen, so of the primary excess air. When the primary excess air is less than 1, an increase of this one generates a reduction of the NO emissions and inversely for the primary excess air upper than 1, the NO emissions increase with this parameter.

The destruction of NO occurs in two different locations. First, N<sub>2</sub> and NO<sub>2</sub> are formed from NO before the secondary air injection. This reduction regenerates NH<sub>3</sub> and occurs in the presence of the radicals NH<sub>2</sub>, NH and NCO. During this phase we notice the preponderance of a reducing atmosphere as well as the radical OH. In the secondary combustion zone the presence of oxygen favours the reduction of NO emissions but also the generation of NO through oxidation of the last incomplete products of combustion. The two different reactions lead to a net increase in the production of N<sub>2</sub>.

The study demonstrates that the NO yield is dependent of the oxygen concentration. The study of the influence of the excess air demonstrate that primary excess air is the predominant parameter because it influences the concentration of NO formed as well as the levels of the reducing species. A primary excess air of one seems to be the most favourable condition since the influence of the secondary excess air is negligible.

## Acknowledgements

The financial support for this work was provided by the Agence De l'Environnement et de la Maitrise de l'Energie (ADEME) and by the Centre de Recherche pour l'Environnement l'Energie et le Déchet (CREED).

## References

- [1] J.P. Olier, Les oxydes d'azote—Préface, Rev. Gén. Therm. 330–331 (1989).
- [2] T. Abbas, P. Costen, F.C. Lockwood, A review of current NO<sub>x</sub> control methodologies for municipal solid waste combustion process, in: 4th European Conference on Industrial Furnaces and Boilers, London, 1997.
- [3] S. Kim, D. Shin, S. Choi, Comparative evaluation of municipal solid waste incinerator designs by flow recirculation, Combust. Flame 106 (1996) 241–251.

- [4] G.G. De Soete, Mécanismes de formation et de destruction des oxydes d'azote dans la combustion, *Rev. Gén. Therm.* 330–331 (1989) 353–373.
- [5] L. Sorum, O. Skreiberg, P. Glarborg, A. Jensen, K.D. Dam Johansen, Formation of NO from combustion of volatiles from municipal solid wastes, *Combust. Flame* 123 (2001) 195–212.
- [6] G.G. De Soete, Overall reaction rates of NO and N<sub>2</sub> formation from fuel nitrogen, in: 15th Symposium International on Combustion, The Combustion Institute, 1974, pp. 1093–1102.
- [7] J.A. Miller, C.T. Bowman, Mechanism and modeling of nitrogen chemistry in combustion, *Progr. Energy Combust. Sci.* 15 (1989) 287–338.
- [8] T. Rogaume, M. Auzanneau, F. Jabouille, J.C. Goudeau, J.L. Torero, The effects of different airflows on the formation of pollutants during waste incineration, *Fuel* 81 (2002) 2277–2288.
- [9] T. Rogaume, M. Auzanneau, F. Jabouille, J.C. Goudeau, J.L. Torero, Computational model to investigate the effect of different airflows on the formation of pollutants during waste incineration, *Combust. Sci. Technol.* 175 (2003) 1501–1533.
- [10] T. Rogaume, F. Jabouille, J.L. Torero, Computational model to investigate the mechanisms of NO<sub>x</sub> formation during waste incineration, *Combust. Sci. Technol.* 176 (2004) 925–943.
- [11] D. Fortsch, F. Kluger, U. Schnell, H. Spliethoff, K.R.G. Hein, A kinetic model for the prediction of NO emissions from combustion of pulverized coal, in: 27th International Symposium on Combustion, The Combustion Institute, 1998, pp. 3037–3044.
- [12] A. Antifora, T. Faravelli, N. Kandamby, E. Ranzi, M. Sala, L. Vigevano, NO<sub>x</sub> emissions from a large scale coal-fired furnace, in: 5th International Conference on Technologies and Combustion for a Clean Environment, 12–15 July 1999, Lisbon, Portugal.
- [13] V. Vitali, V. Lissianski, V.M. Zamansky, P.M. Maly, M.S. Sheldon, Optimisation of advanced reburning via modeling, in: 28th International Symposium on Combustion, The Combustion Institute, 2000, pp. 2475–2482.
- [14] S. Goel, A. Sarofim, P. Kilpinen, M. Hupa, Emissions of nitrogen oxides from circulating fluidised bed combustors: modeling results using detailed chemistry, in: 27th International Symposium on Combustion, The Combustion Institute, 1996, pp. 3317–3324.
- [15] R.J. Kee, F.M. Rupley, J.A. Miller, Chemkin-II: a Fortran chemical kinetics package for the analysis of gas-phase chemical kinetics, Sandia Report 89-8009B, 1989.
- [16] P. Glarborg, D.-J. Alzueta, J.A. Miller, Kinetic modeling of hydrocarbons/nitric oxide interactions in a flow reactor, *Combust. Flame* 115 (1998) 1–27.
- [17] GRI-MECH, Version 3-11, <http://www.me.berkeley.edu/gri-mech/>, 1999.
- [18] P. Dagaut, J. Luche, M. Cathonnet, The kinetics of C<sub>1</sub> to C<sub>4</sub> hydrocarbons–NO interactions in relation with reburning, in: 28th International Symposium on Combustion, The Combustion Institute, 2000, pp. 2459–2466.
- [19] F. Hahnel, Conception d'un réacteur à lit fluidisé pour l'étude de l'incinération de déchets. Application à l'étude des mécanismes de transformation de l'azote lors de la combustion du polyamide-6,6, Thèse de doctorat de l'Université de Haute-Alsace, 1999.
- [20] P. Glarborg, R.J. Kee, J.A. Grcar & Miller, PSR: a Fortran program for modeling well-stirred reactors, Sandia Report 86-8209, 1986.